Available online at www.sciencedirect.com

SciVerse ScienceDirect

Scripta Materialia 68 (2013) 179–182

Scripta MATERIALIA

www.elsevier.com/locate/scriptamat

Enhanced superplasticity and diffusional creep in ultrafine-grained Mg–6Al–1Zn alloy with high thermal stability

W.J. Kim* and I.B. Park

Materials Science and Engineering, Hongik University, 72-1 Mapo-gu, Sangsu-dong, Seoul 121-791, Republic of Korea

Received 30 July 2012; revised 18 September 2012; accepted 8 October 2012
Available online 13 October 2012

Ultrafine-grained Mg–6Al–1Zn alloys, which have β-$Mg_{17}Al_{12}$ 70–140 nm particles preferentially located at the grain boundaries, exhibited excellent thermal stability and superplasticity at high temperatures. Diffusional creep (Coble creep), which has rarely been reported in other ultrafine-grained Mg alloys and composites, becomes dominant over the grain boundary sliding mechanism at strain rates near 10^{-4} s^{-1} at 523–573 K.

Keywords: Severe plastic deformation; Magnesium alloys; Superplasticity; Grain refining; Ultrafine-grained microstructure

A small grain size and high thermal stability are the two most important factors for enhancing superplasticity in materials. Severe plastic deformation (SPD) techniques, including equal-channel angular pressing (ECAP) and high-pressure torsion (HPT), have proved effective in the grain refinement of many Mg alloys [1–4]. The materials processed by these methods exhibit superplasticity at low temperatures ($\leqslant 0.5T_m$, where T_m is the melting temperature) due to enhanced grain boundary sliding (GBS) because of the ultrafine grains. However, the microstructures of the processed materials often have low thermal stability at temperatures $\geqslant 0.5T_m$; therefore, obtaining superplasticity at high strain rates and low flow stresses, which is required in the superplastic forming industry, is difficult.

Recently, Kim et al. [5] reported that ZK60 (Mg–Zn–Zr) alloy processed by high-ratio differential speed rolling (HRDSR), which is a SPD method applicable to materials in sheet form, could exhibit superplasticity at high strain rates and high temperatures comparable to that of its powder-metallurgy counterpart. During processing, dynamic precipitation of a high density of nano-sized $MgZn_2$ particles with an average size of 32 nm preferentially occurred on the boundaries of the ultrafine-grained (UFG) grains, which resulted in significant enhancement of the thermal stability. This material will be hereafter referred to as HRDSR ZK60. By using a similar concept and technique, we also succeeded in developing a very fine-grained (1.1–1.5 μm) microstructure containing very fine β-$Mg_{17}Al_{12}$ phase particles 70–140 nm in size on the grain boundaries in AZ61 (Mg–Al–Zn) alloys [6,7].

In this study, superplasticity and deformation mechanisms of these UFG AZ61 alloys were examined. For comparison, the superplasticity of UFG AZ31 alloy with a very small volume fraction of β-$Mg_{17}Al_{12}$ phase particles [8] was also examined. Superplastic properties of these materials were compared with those of Mg–9Al alloy processed by ECAP [3] and AZ61 alloy [4] processed by HPT. In addition, we discuss the appearance of a region where diffusional flow governs the plastic flow in the HRDSR-processed AZ61 alloy, which has been rarely observed in other UFG Mg alloys and composites processed using SPD or powder metallurgy.

Commercial AZ61 (Mg–6Al–1Zn) alloy sheets 1.6 mm thick were used as the starting material in this study. The material had a mean grain size of 15 μm and a highly solid solutionized matrix [6]. HRDSR was performed using a rolling mill with a roll diameter of 300 mm. The speed ratio between the upper and lower rolls was set at 2 (6 rpm:3 rpm) or 3 (9 rpm:3 rpm). A cold AZ61 sheet was fed into the hot rolls (423 K) for a total reduction in thickness of 66% or 67% through a two-step rolling process. The sheet was rolled to 1.1 mm and then rolled again to a final thickness of 0.55 or 0.53 mm. There was no rotation of the samples between the passes. The two resultant materials will

* Corresponding author. Tel.: +82 2 320 1468; fax: +82 2 325 6116; e-mail: kimwj@wow.hongik.ac.kr

1359-6462/$ - see front matter © 2012 Acta Materialia Inc. Published by Elsevier Ltd. All rights reserved.
http://dx.doi.org/10.1016/j.scriptamat.2012.10.011

hereafter be referred to as HRDSR AZ61R2 and HRDSR AZ61R3, respectively. The AZ31 (Mg–3Al–1Zn) alloy was also processed using similar procedures, and the details of these procedures are available in Ref. [8]. This material will be hereafter referred to as HRDSR AZ31.

For the microstructure study, the transverse direction–rolling direction planes of the samples were examined by field emission transmission electron microscopy (TEM, JEM 2001F, 200 kV) equipped with an energy dispersive X-ray spectrometer. The particle and grain-size measurements were performed with the aid of image analysis software (Olympus analySIS TS Material®). For tensile testing at high temperatures, tensile specimens with a dog-bone geometry and a 5 mm gauge length were used. Tensile elongation-to-failure tests were performed under constant-crosshead-speed conditions to evaluate tensile ductility at several temperatures and strain rates. The strain rate change (SRC) tests were carried out at various temperatures between 473 and 573 K. A prestrain of $\varepsilon = 0.12$ was imposed at an initial strain rate of $4 \times 10^{-3}\ s^{-1}$ before the SRC was applied to stabilize the microstructure. A strain of ~0.03 was applied between the strain rates followed by the prestraining. The SRC test at each temperature was repeated twice. This repetition was conducted to confirm that the strain rate–stress relation obtained from the SRC test was reliable. In the case of HRDSR AZ61R3, additional SRC tests were applied in the narrow crosshead speed ranges between 0.05 and 0.15 min s^{-1} (1.67×10^{-4} and $5 \times 10^{-4}\ s^{-1}$ in initial strain rate) and between 0.15 and 0.3 min s^{-1} (5×10^{-4} and $1 \times 10^{-3}\ s^{-1}$) at 523 K to measure the values of the local strain-rate sensitivity (m) as a function of strain. During the SRC and elongation-to-failure testing, the tensile jig was preheated and then the sample was mounted onto the sample holder. To reach the designated temperature, 5 min was required. The sample was then allowed to equilibrate at the desired temperature for an additional 5 min before initiating straining.

HRDSR AZ61R3 exhibits a microstructure that consists of fine equiaxed grains ($L = 1.1$ μm, where L is the linear intercept grain size) and tiny β-$Mg_{17}Al_{12}$ particles ($d_p = 70$ nm, where d_p is the average size) that are preferentially located at the grain boundaries (Fig. 1a). The microstructure of HRDSR AZ61R2 (Fig. 1b) is relatively coarser ($L = 1.5$ μm and $d_p = 140$ nm), but many β-particles are also concentrated at the grain boundaries. The formation of smaller grain and particles sizes in HRDSR AZ61R3 is most likely a result of the accumulation of a higher shear strain at a higher speed ratio and a shorter available time for the diffusion-related spheroidization of β particles at a higher speed. HRDSR AZ31 has a submicron grain size ($L = 0.6$ μm), but in contrast to the two HRDSR-processed AZ61 alloys, the volume fraction of the β phase is very low (Fig. 1c). The HRDSR ZK60 alloy shows that $L = 0.6$ μm, and the grain boundaries are heavily decorated with a high density of nanosized particles ($MgZn_2$) with $d_p = 32$ nm (Fig. 1d).

The results from the SRC tests for HRDSR AZ61R3, HRDSR AZ61R2 and HRDSR AZ31 performed at 523 K, which are presented as double-log plots of $\dot{\varepsilon}$ vs. σ (where $\dot{\varepsilon}$ is the strain rate and σ is the flow stress), are shown in Figure 2a. As indicated for each material, the data from the second SRC round are reasonably close to those from the first SRC round, and the m values measured during the first and second rounds are similar. This result indicates that the microstructure change during the SRC tests was minimal.

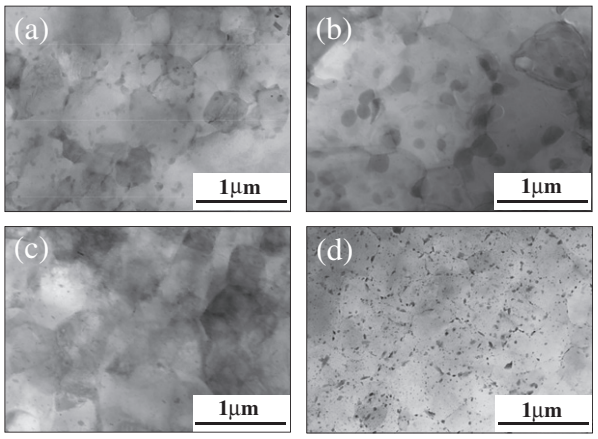

Figure 1. TEM micrographs of (a) HRDSR AZ61R3, (b) HRDSR AZ61R2, (c) HRDSR AZ31 and (d) HRDSR ZK60.

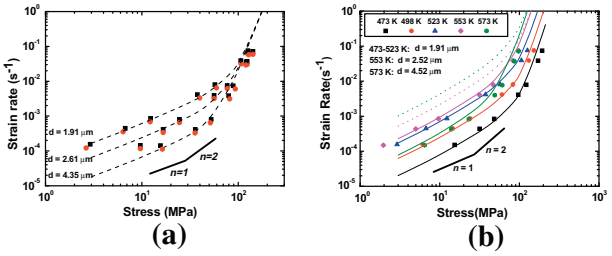

Figure 2. (a) The SRC data of HRDSR AZ61R2, HRDSR AZ61R3 and HRDSR AZ31 at 523 K (solid squares and solid circles represent the first and the second loops in the SRC testing, respectively). The dotted curves are the strain rate–stress curves calculated using Eq. (1) for the best fit to the experimental data. (b) The SRC data of HRDSR AZ61R3 at different temperatures. The solid curves at different temperatures were constructed using Eq. (1) for the best fit to the experimental data. The dotted curves represent the prediction at 553 and 573 K at the initial grain size of HRDSR AZ61R3.

Figure 2b shows the SRC results for HRDSR AZ61R3 at various temperatures. In this plot, the inverse of the slope of the curves represents the strain-rate sensitivity exponent ($m = 1/n$, where n is the stress exponent). The m value measured at strain rates below $10^{-3}\ s^{-1}$ increases as temperature increases; it is 0.5~0.6 at 473 K, but it is ~0.8 at 523–573 K. The SRC tests performed at 523 K in the narrow strain-rate ranges between 1.67×10^{-4} and $5 \times 10^{-4}\ s^{-1}$ and between 5×10^{-4} and $1 \times 10^{-3}\ s^{-1}$ indicate that the m values are 0.48–0.49 and 0.78–0.81, respectively, and these high m values can be maintained at least up to a strain of 0.86 (Fig. 3a). Above SRC results suggest that contribution of diffusional flow to the plastic flow increases as temperature increases and strain rate decreases. In the SRC testing in the strain rate range between 1.67×10^{-4} and $5 \times 10^{-4}\ s^{-1}$ (Fig. 3a), the m value